An Experimental Study of Short-Circuit Current Making Operation of Air Medium-Voltage Load Break Switches

Naghme Dorraki, and Kaveh Niayesh, *Senior Member, IEEE*

***Abstract*— Replacing SF_6, the most potent greenhouse gas, with an alternative gas is a challenge faced by medium-voltage load break switches (MV-LBS). Air is a possible alternative, but there are some challenges regarding low dielectric strength leading to high arcing time and dissipated energy. Therefore, understanding the switching processes for both interruption and making operations in air MV-LBS is crucial to designing efficient compact switchgear.**

This work focuses on making operations in air MV-LBS. A synthetic test circuit and a model switch are designed based on the standards to simulate making operations under fault conditions similar to a real test. The test condition is set to achieve high pre-strike arcing time and energy. The results show that the most destructive impact of the making short-circuit current occurs in the first half-cycle of the load current when the pre-strike arc is formed. With an average short-circuit current with a peak of 22 kA and a breakdown voltage of 20 kV, the switch failed to re-open due to the arcing contacts welding after four successive making operations without main contacts and seven successive operations with main contacts. It has been shown that the total arcing contact mass loss occurs mainly during the pre-arcing time. Increasing the closing speed could be a possible solution to minimize the impact of arcing.

***Index Terms*—medium voltage (MV), load break switch (LBS),** making **operations, contacts erosion, arcing contacts, main contacts, arc erosion.**

I. Introduction

System and component development are the prerequisites for evolution in future distribution networks. A high number of successful and reliable operations is required for gas-insulated switchgear (GIS), while the use of SF_6 has been or is going to be banned because of its environmental impact. The California Air Resource Board (CARB) has planned to start SF_6 phase-out in 2025, and European countries have aimed to cut the F-gas emission by two-thirds by 2030 compared to 2014 [1].

So far, SF_6 has been the most efficient insulation gas for arc-based switchgear because of its high dielectric strength and its superior thermal properties leading to an outstanding arc quenching performance. SF_6 alternatives should be chosen to lead the switch design to be compact and efficient at an affordable price. CO_2 is one of the alternatives in a mixture with N_2, F-Ketones, or F-Nitriles, providing reasonable interrupting performance [2-5]. However, this is still not as good as SF_6 based interrupters. Air and air mixtures are considered as other solutions [5, 6]. Air as a cost-efficient alternative to SF_6 has a dielectric strength of approximately one-third of SF_6 at atmospheric pressure, which needs a larger interrupter with a higher gas pressure for a successful interruption performance. Therefore, a total change in the design of SF_6-based switchgears is necessary to make them compatible with air as the insulation gas.

Replacing SF_6 with air as insulation gas in a medium voltage load break switch (MV-LBS) with a compact design based on SF_6 features is challenging. According to IEC 62271-200 [7], medium voltage is generally applied to voltages above 1 kV up to 52 kV. The most common rated operation voltages for MV-LBS are 12 kV, 24 kV and 36 kV. MV-LBS at the rated operation voltages should be designed to successfully interrupt load currents up to 1250 A and withstand short-circuit currents of tens of kiloamperes in the making operation. Evaluating the performance of air-based MV-LBS is essential to reach a practical and cost-efficient design. A number of studies have been performed on interruption performance. Ablation-assisted current interruption and investigation on airflow, contacts, nozzle material and geometries at different switching conditions have been studied to understand the process and find an appropriate design for a successful current interruption for air-based MV-LBS [8-10]. In addition to load current interruption, the switch should be able to withstand different fault conditions.

Short-circuit current levels could be increased by the reinforced network structure. Furthermore, a reduction in network losses leads to larger DC-time constants of the short-circuit current, leading to larger peak values of the fault current. Therefore, the switch should be able to pass short-circuit currents of tens of kiloamperes while closing and be able to re-open for the next operation. While the distance between the contacts is decreasing by closing the switch, a breakdown occurs at a specific distance due to the potential difference across the switch which results in ignition of a pre-strike arc. The short-circuit current flows through the arc column before contacts being fully closed. The dissipated arc energy could be partly absorbed by the contacts' surfaces, resulting in the contact surfaces melting and evaporating. Subsequently, the contacts with melted surfaces could be welded in the closed

This work was supported by the Norwegian Research Council under Grant 269361. *(Corresponding author: Naghme Dorraki.)*

N. Dorraki and K. Niayesh are with the Department of Electric Power Engineering, Norwegian University of Science and Technology, 7491 Trondheim, Norway (e-mail: naghme.dorraki@ntnu.no, kaveh.niayesh@ntnu.no).

position when the majority of fault current passes through them, preventing the switch from re-opening [11]. Since air as an insulation gas alternative to SF_6 has lower dielectric strength, a higher arcing and larger dissipated energy in the pre-strike arc are expected. Therefore, the impact analysis of making operation for air-based MV-LBS is crucial for optimizing the switch design and estimation of its lifetime. Although there are several studies on electrical contacts erosion as a consequence of arc [12-14], there is still a research gap in understanding the erosion mechanisms of sliding contacts under short-circuit conditions. Pre-strike arcing between the contacts sliding through each other with molten surfaces while passing short-circuit current of kiloamperes represents a complicated case, which has not been investigated thoroughly in the literature. This is not only the case in MV-LBS, but also in earthing switches used in power switchgear. Therefore, understanding the switch behavior during making operation is crucial to avoid switch failure because of contacts welding.

The erosion of electrical contacts exposed to an arc has been shown to be dependent on the contacts material, structure, and geometry. Composite contact materials tend to have higher erosion than pure material due to problems regarding the processing technique, grain size, and impurities [12, 15, 16]. Understanding the mechanism responsible for the increase in erosion requires investigating the switching processes under different test conditions. The purpose of this article is a laboratory assessment of the air-based MV-LBS in making operations for different fault conditions. A synthetic test circuit is established, and a test object similar to the commercial model is designed. The analysis of the switching behavior is presented, including the role of arcing and main contacts in switch failure due to erosion/welding at different short-circuit current levels and closing speeds. The ohmic losses when the contacts with molten surfaces are sliding though each other are also evaluated to extend the results to longer short-circuit.

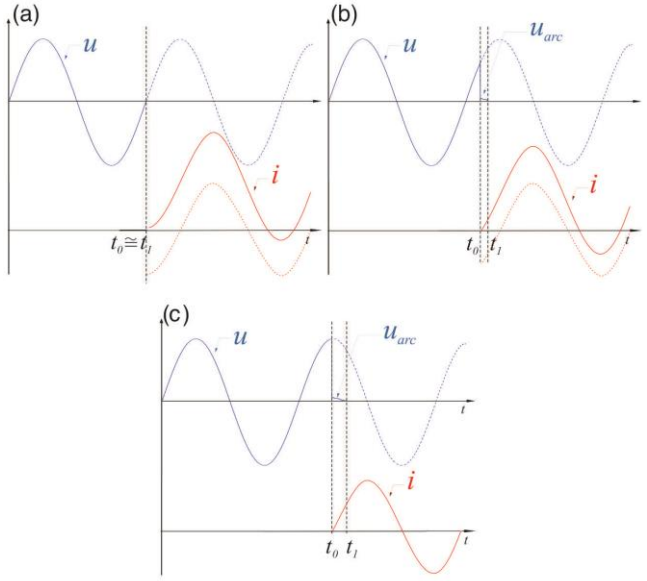

Figure 1. Three typical cases for the moment when the switch is closed; (a) asymmetrical making operation with negligible arc energy (b) randomly moment of closing (c) symmetrical making operation with high arc energy

II. Experiment Method

In this section, the method and technique for evaluating the switch behavior under fault conditions are described.

A. Synthetic test circuit

The experiments are designed to achieve the highest level of arc energy to investigate the effect of pre-strike arc on the switch malfunction. The switch could be subjected to different arcing times, depending on the moment of closing. In real-world applications, the switch could be closed at each phase of the power-frequency voltage. Figure 1 shows current and voltage waveforms in a real making operation at three different closing moments. If the switch closes when the applied voltage is zero, an asymmetrical network frequency current passes through the switch, shown in Figure 1 (a). In this case, the arc energy is negligible, but the largest current amplitude flows through the switch, this is called high current case. In contrast, if the breakdown occurs at the peak of the applied voltage, a symmetrical network frequency current passes through the switch. In this case, the largest possible arc energy is dissipated between the contacts, this is called high-energy case (see Figure 1 (c), where *u* is the network voltage, and *i* is the making current). The pre-strike arc burns in the time interval between t_0 and t_1; the breakdown occurs at t_0, and the switch is closed at t_1. Figure 1 (b) shows a random moment of closing operation. The current waveshape is between the cases shown in Figure 1 (a) and (c), so that the maximum current is less than case (a), and the maximum energy is less than the case (c).

To simulate the real-world making operation in laboratory, a synthetic test circuit for the making operation according to IEC 62271-101 is established [17]. In this case, the high energy test is performed, which corresponds to the largest energy dissipation in the making switching arc. The schematic of the synthetic test circuit is shown in Figure 2. The circuit consists of two parts, the high current circuit and the high voltage one. The high current part includes a high-power transformer which can supply network frequency short-circuit currents of tents of kiloamperes. The high voltage circuit subjects the test object to the operation voltage by energizing the charged capacitor. The capacitor is charged to the operation voltage by the DC high voltage power supply. Once charged, switch S_1 is disconnected. A pre-strike arc ignites between the contacts due to dielectric breakdown while closing the switch. Immediately after the breakdown, a signal will be sent to the trigger vacuum switch (TVS) and the high current circuit injects one half-cycle of the 50 Hz short circuit current by connecting the transformer output

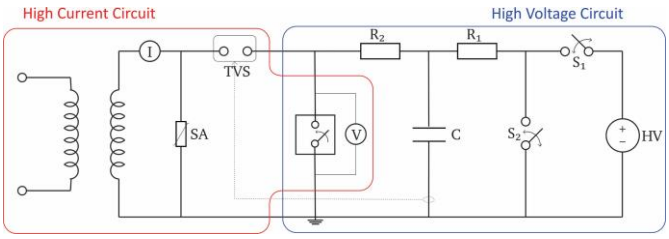

Figure 2. Schematic of the synthetic test circuit for performing the making operation.

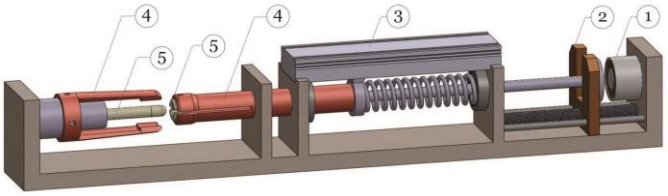

Figure 3. Spring-type test object; (1) Solenoid magnet, (2) Contacts' separator, (3) Position sensor, (4) Main contacts, and (5) Arcing contacts.

to the test object. The time delay between the detection of a current flow caused by breakdown of the switch and connection of the high current circuit is less than 50 µs. Switch S_2 is open during the making test and is closed when the test is over for the sake of safety. A 6015A Tektronix voltage probe together with TDS2014B Tektronix oscilloscope 8-bit measure the arc voltage. The time resolution of the measurements has been 4 µs, and a Rogowski coil measures the arc current. An additional voltage measurement is used to measure the charging voltage of the capacitor. The combination of both measurements is shown in Figure 5.

The experiments are designed based on the third case (Figure 2 C) at the breakdown voltage of 20 kV, equivalent to the peak of the rated voltage of a 24 kV MV-LBS. It has to be mentioned that there is some uncertainty in having the breakdown precisely on the peak of applied voltage because of the system synchronization accuracy of ±0.001 s, and the random behavior of arc ignition due to the eroded contact surfaces. Therefore, there is a slight difference in di/dt under the same test conditions.

B. Test Object

A spring-type drive mechanism is designed as the test object. A schematic of the test object is shown in Figure 3. The moment of breakdown is adjusted by triggering the solenoid magnet to release the dynamic contact. A position sensor records the movement of the contacts. The arcing contacts include a pin with a diameter of 10 mm and a split tulip with an outer diameter of 20 mm and an inner diameter slightly less than 10 mm to provide full touch in the closed position. The arcing contacts are made of copper/tungsten (20/80), and the clamp-shaped main contacts are made of copper. The main contacts are fixed for all the tests and four pairs of arcing contacts have been examined for different test conditions.

The contacts' material and the closing speed of ~3 m/s are chosen for the model switch not to be too different from the commercial switches. A higher closing speed can shorten the arcing time and reduce the arc energy, while keeping the other design parameters constant. By adjusting the spring length, a higher closing speed of ~ 4 m/s is realized in order to analyze to what extent an increased closing speed would reduce the destructive effects of the making operation on the switch.

A typical travel curve of the dynamic contact is shown in Figure 4. Mechanical closing of the switch without applying any current shows an average speed of ~ 4 m/s (blue dashed line), while passing the short-circuit current reduces the closing speed as indicated by the change in the steepness of the travel curve (blue solid line). The deviation is due to electrodynamics' forces made by the high short-circuit current and the forces caused by the pressure increase due to the pre-strike arc acting against the switch closing.

The making operation under a short-circuit current could be divided into three main intervals based on the contact movement. This helps to better understand the applied stresses on the switch at different stages of the making operation. The time from releasing the contact by the solenoid magnet (t_0) to the arc ignition in between the contact (t_1) is considered as a high-voltage interval. From the breakdown time until the arcing contacts touch (t_2) is called the pre-arcing interval. The latching interval is the time from t_2 when the arc seizes as the contacts touch to the time of full closure of the switch (t_5). t_3 is the moment when the main contacts meet. t_4 is the zero-crossing of the short-circuit current. The time interval between t_2 and t_3 is considered a part of the latching interval when no arc exists. The short-circuit current passes through the arc column between the arcing contacts in pre-arcing interval. The arc contacts, however, carry a small fraction of the short circuit current in the main part of the latching interval (in the time period from t_3 to t_4) when the arcing and main contacts are both closed.

The experiments are designed to investigate the making performance of the switch at different closing speeds and levels of short-circuit current. The applied voltage of 20 kV is chosen as the breakdown voltage for all the tests, which is equivalent to the peak of the rated voltage for MV-LBS. All the tests have been repeated for four different samples to reduce the measurement error. To distinguish the role of arcing contacts and main contacts, all the tests have been repeated with and without main contacts. The total average arcing contacts (pin+tulip) are ~52 g. Therefore, the contacts mass loss is measured with a precise scale with accuracy of ±0.00001 g. To avoid the contacts being contaminated during the process, each pair of contacts were kept in a separate enclosure. No specific cleaning procedure was used in order to be close to the real operation. The total arc energy and effective arc energy close to

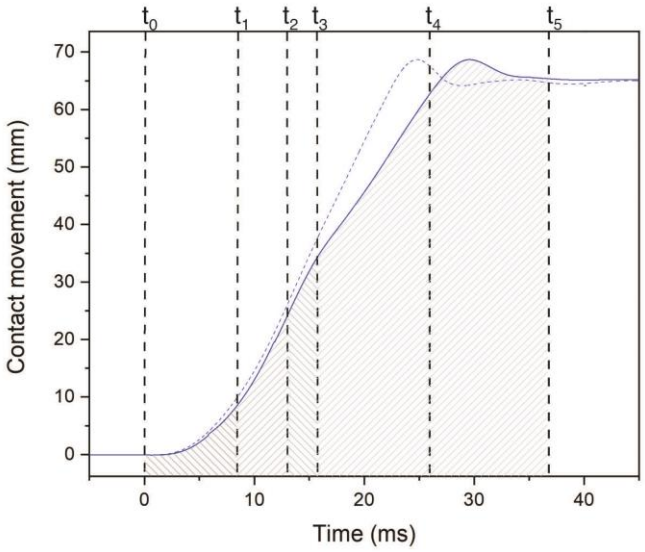

Figure 4. Travel curve of the dynamic contact with a closing speed of ~4 m/s, divided into main operation intervals based on IEC 62271-101; the high-voltage interval (t0-t1), pre-arcing interval (t1-t2), and latching interval (t2-t5).

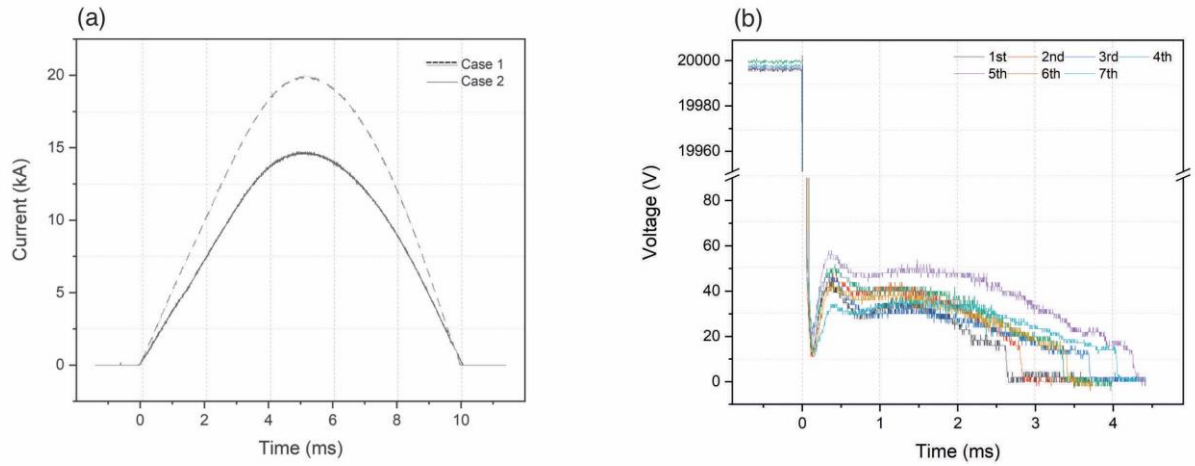

Figure 5. Half-cycle 50 Hz short circuit current with a peak of 14.8 and 20.2 kA (a), Arc voltage measurements for seven successive tests (b).

the surface of the contacts are measured for each test to evaluate the switch operation under the specific fault condition.

III. Results

In this section the results regarding pre-strike arcing and contacts erosion are presented to find the interrelation between fault conditions, operational parameters, and the switch wear.

A. Arc energy

The arc voltage and current are directly measured for each test. Because of the 1 ms jitter of the test object, there is a slight difference in di/dt for different tests under the same conditions. In this case, the first half-cycle of the current waveforms differs slightly. It is, however, negligible for the calculation of pre-strike arc energy since the arc current does not vary considerably in the pre-arcing interval. Depending on the series inductance in the primary side of the transformer, the amplitude of the short circuit current can be adjusted. Figure 5 (a) shows half-cycle 50 Hz current waveforms considered as two short-circuit current levels used in the experiments. Figure 5 (b) shows arc voltage waveforms for a series of making tests on one pair of arcing contacts under the short circuit current of case 1. All the voltage waveforms show a sharp fall from the dielectric breakdown voltage at 20 kV to the arc voltage, which is in the order of tens of volts. The first 50 µs of the voltage fall is neglected due to interference with electromagnetic noises caused by air breakdown. An increase in the arc voltage is recorded followed by a gradual decay in the waveform. The increase in the arc voltage shows the difference between static and dynamic arcs. As previously mentioned in pre-strike arc characteristics [18], the peak in arc voltage belongs to the stage when the pre-strike arc stabilizes in the center while the contacts are closing. A rapid decrease from ~ 18 V to zero is observed in all the voltage waveforms at the time of arc contact closure, which refers to the minimum arcing voltage, i.e., the anodic plus cathodic voltage drop for tungsten/copper (80/20) [15, 19]. The pre-strike arc duration is measured based on the voltage waveform from the moment of breakdown to voltage zero,

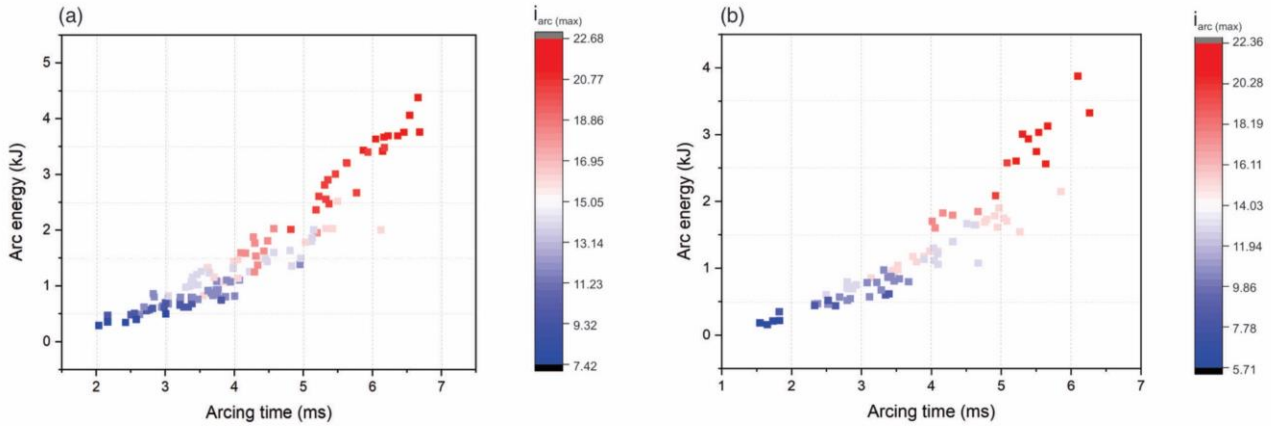

Figure 6. Pre-strike arc energy as a fuction of arcing time for different level of short-circuit current at the touching moment of arcing contacts for two closing speed of (a) 3 m/s and (b) 4 m/s.

equivalent to the pre-arcing interval. Since it is only possible to measure the arc current and voltage over the electrical contacts, the arc energy is estimated by the following equation:

$$E = \int_{t_1}^{t_2} i_{arc}(t) \,.\, u_{arc}(t)\, dt \qquad (1)$$

A series of operations are performed for two closing speeds of 3 and 4 m/s for four different samples. The making test is repeated on each until the switch fails to re-open due to the arcing contacts welding. The arcing time and energy are calculated for each specific test. Figure 6 shows the interrelation between the dissipated arc energy and arcing time for different short-circuit current values at the touching moment of the arcing contacts (t_2-Fig.4). It can be seen that the dissipated arc energy is increasing with both the arcing time and the part of short-circuit current that passes through the arc column before the arcing contacts touch (pre-arcing interval).

B. Mass loss

The rate of contacts' mass loss could provide information on the switch service life prediction. The difference in the mass loss at each test and the total mass loss are measured to identify the erosion rate under different fault conditions. After each test, the arcing contacts have been removed to be weighed and reinstalled for the next operation. The reproducibility of the tests has been examined for four different samples. The making test is repeated on one sample until welding of the arcing contacts occurs. Some previous investigations considered the total arc energy involved in the contacts' mass loss including cathode/anode fall energy, radiations, the energy of neutral atoms [15] [20, 21]. However, there are some other studies that presented the mass loss as a function of cathode/anode fall energy [12, 22]. Due to the complexity of distinguishing different energy components, it is still controversial to present each energy component contribution in contact wear. To perform a comparative analysis, both cases are evaluated with/without the main contacts. The arc energy close to the surface of the contacts is estimated by the following equation:

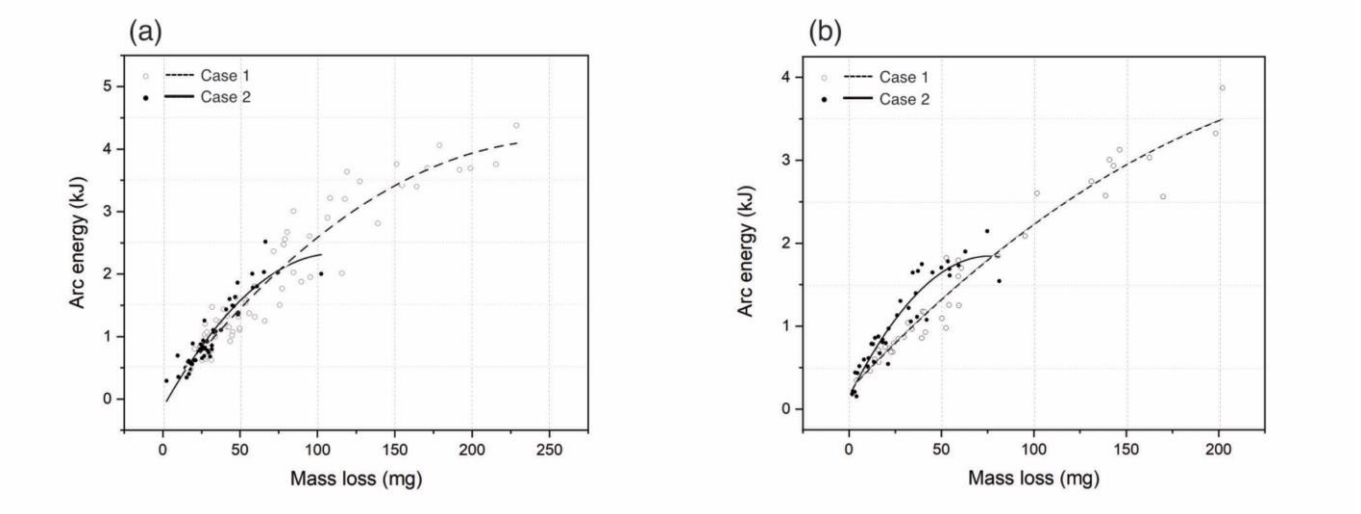

Figure 7. The mass erosion rate as a function of pre-strike arc energy for a series of operations with (a) and without (b) main contacts.

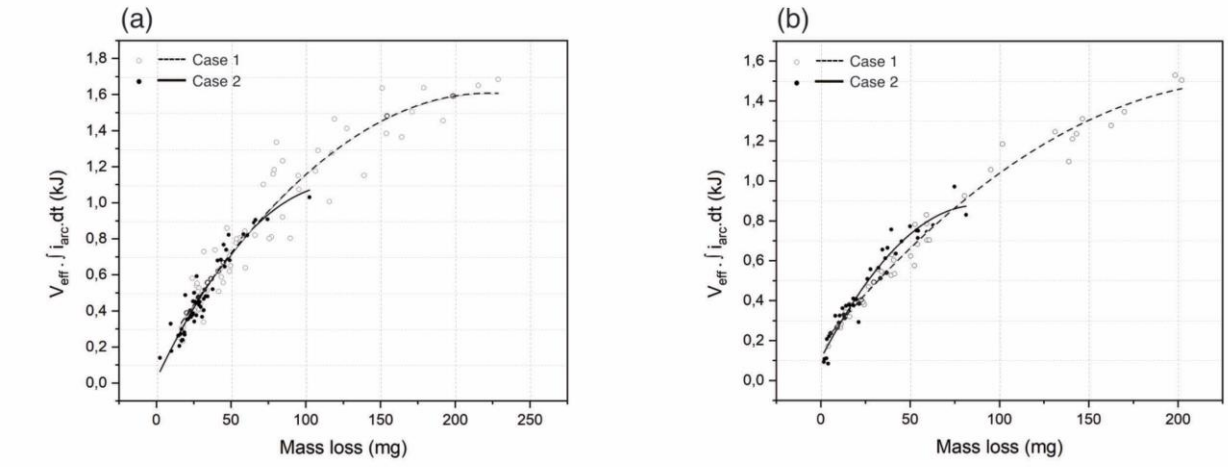

Figure 8. The mass erosion rate as a function of electrodes fall energy for a series of operations with (a) and without (b) main contacts.

$$E_{C/A} = \int_{t_1}^{t_2} \Delta U_{eff} \ . i_{arc}(t)\, dt \qquad (2)$$

where ΔU_{eff} is sum of the effective voltages for cathode and anode presented by equations (3) and (4), respectively [12].

$$\Delta U_{eff-} = \Delta U_{cathode} - \left(\frac{5}{2}\frac{kT_e}{e} + \frac{\phi}{e}\right) \qquad (3)$$

$$\Delta U_{eff+} = \Delta U_{anode} - \left(\frac{5}{2}\frac{k(T_p - T_e)}{e} + \frac{\phi}{e}\right) \qquad (4)$$

T_e, T_p, and T_a are the electron, plasma, and anode surface temperatures. ϕ is the work function. Since $T_e \approx (T_p - T_a)$, the effective electrode voltage is defined as:

$$\Delta U_{eff} = \Delta U_{cathode} + \Delta U_{anode} \approx 18 \qquad (5)$$

The electrodes voltage fall for tungsten/copper(80/20) is approximately constant 18 V. A series of tests were performed with and without main contacts for both closing speeds to show the role of main contacts on reducing the rate of contacts erosion. The difference in mass loss versus the total arc energy (equation. 1) and the electrode fall energy (equation. 2) are evaluated for arcing contacts during making operation with/without main contacts in Figure 7 and Figure 8, respectively. For both cases, an increase in the energy leads to more mass loss, while the total arc energy is significantly higher than electrode fall energy.

To identify the effect of main contacts on the prolongation of the switch life time, a series of tests were repeated on each sample with and without main contacts until switch failure due to contacts welding. Figure 9 and Figure 10 show the total mass loss of the arcing contacts by repeating the making test with and without main contacts, respectively. The mass loss varies a lot in some of the tests, while the average shows a meaningful erosion rate in the series of the experiments. The variation could be due to the difference in the dissipated arc energy because of

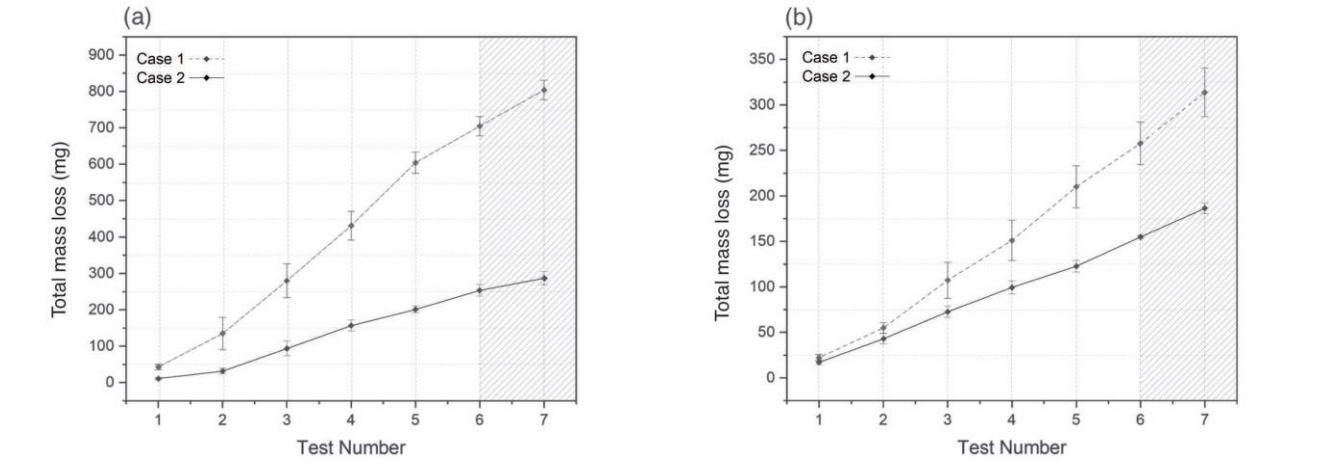

Figure 9. Mass loss from arcing contacts with main contacts in the model switch for two cases of short-circuit current at a closing speed of (a) 3 m/s, and (b) 4 m/s. The shaded parts show the tests where erosion on the main contacts is observed.

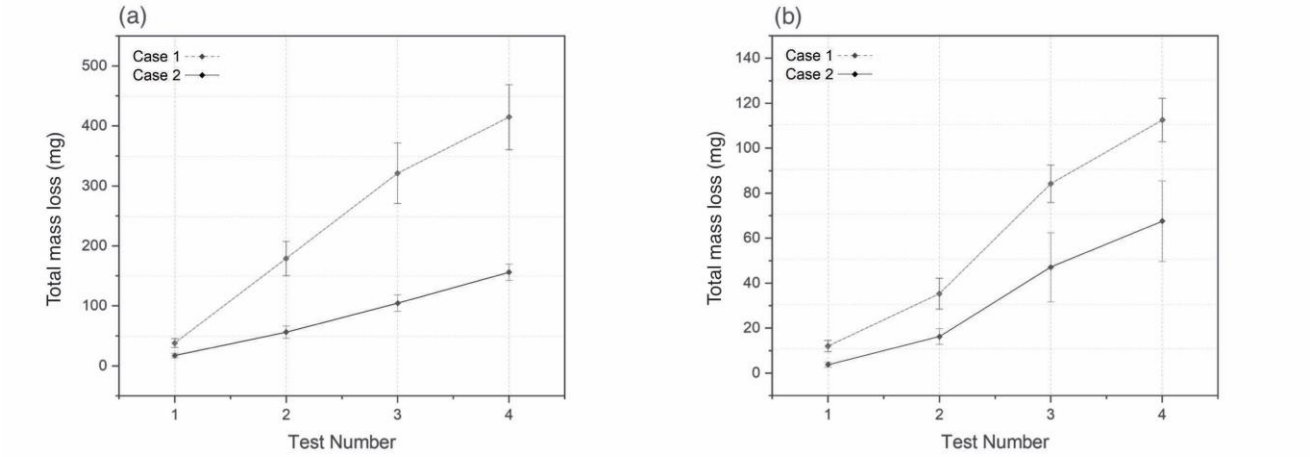

Figure 10. Mass loss from arcing contacts without main contacts in the model switch for two cases of short-circuit current at closing speed of (a) 3 m/s, and (b) 4 m/s.

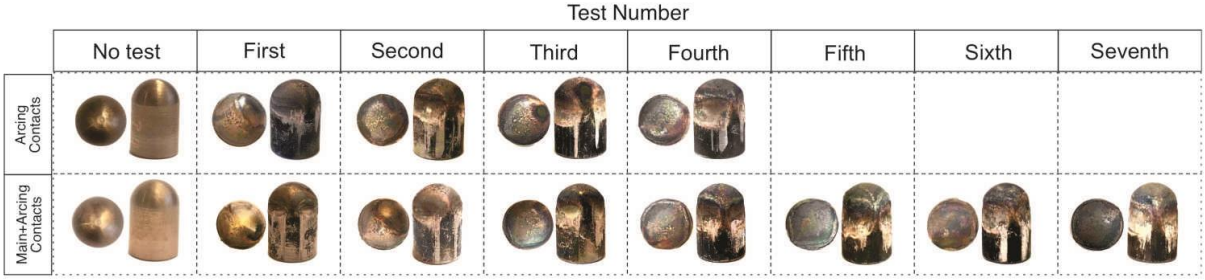

Figure 11. Arcing contacts' degradation after repeating the making test 4 times without main contacts and 7 times with main contacts. Both in case 1 with a closing speed of 3 m/s.

the random arc ignition on the eroded surfaces. The total mass loss is measured after each test for two cases presented in Figure 5 The average short-circuit current is higher for case 1 compared to case 2. For the model switch, including arcing and main contacts at a closing speed of 3 m/s, the making test was repeated six times on one sample to record the first contacts welding for case 1. Two more samples out of the remaining three were welded after the seventh making test in case 1 with a 3 m/s closing speed. Some erosions on the main contacts have been observed at this step besides the arcing contacts welding. The shaded regions in Figure 9 show the making tests where erosion on the main contacts is observed. At the closing speed of 4 m/s, the increase rate of the total mass loss is slower than 3 m/s for both cases, which means the switch can withstand a higher number of making operations. For the model switch including the arcing contacts (without the main contacts), the switch failed to re-open upon three out of four samples after the fourth test in case 1, with a closing speed of 3 m/s. The recorded total mass loss resulting in contacts welding at closing speed of 3 m/s is about three times higher compared to the tests under the same conditions at the closing speed of 4 m/s. The highest mass loss is recorded for case 1, with a higher short-circuit current compared to case 2.

C. Arcing contacts degradation

By repeating the making operation on one pair of arcing contacts, more contact wear is observed. Higher pre-strike arcing time and dissipated energy lead to higher contacts erosion. *Figure 11*shows the arcing contacts' (cathode) degradation for the tests with and without main contacts. The intermediate states after each test are shown and these ended up welding after four operations without main contacts and after seven operations with main contacts at a short-circuit current in case 1 and a closing speed of 3 m/s. The images illustrate rough and uneven surfaces with fissures and pitting. A gradual decrease in the pin width is observed by repeating the making operation. For these two cases, the total mass loss resulting in contacts welding with and without main contacts is reported 831.3 and 445.1 mg, respectively.

IV. Discussion

For MV-LBS during the making operation under a fault condition, the arcing contacts erosion starts in the pre-arcing interval when the dissipated arc energy is partly absorbed by the contacts' surfaces, resulting in their melting and evaporation. The results show that the probability of switch failure due to contacts welding increases by more erosion in arcing contacts where the contacts' mass loss increases by absorbing dissipated arc energy during the pre-arcing interval (Figure 9 and Figure 10). It can be inferred that the pre-strike arcing causes contact surface melting. However, it is controversial whether the total dissipated arc energy should be considered as a factor of contacts erosion or the energy close to the surface of contacts regarding the cathodic and anodic voltage fall (electrode fall energy). Figure 7 and Figure 8 show the variation of the total arc energy and electrodes fall energy with the electrodes mass loss. It can be inferred that the variation of total dissipated arc energy is more pronounced than the electrode fall energy with the increase in the electrodes mass loss and there is a significant difference between them in high rate of mass loss. The correlation between mass loss and total arc energy is very good with a non-linear correlation coefficient of 0.97. The calculated non-linear correlation coefficient between electrode fall energy and mass loss was 0.93, which indicates that this parameter can also be used for the mass loss determination almost as good as the total energy. Besides, it can be seen that the same amount of

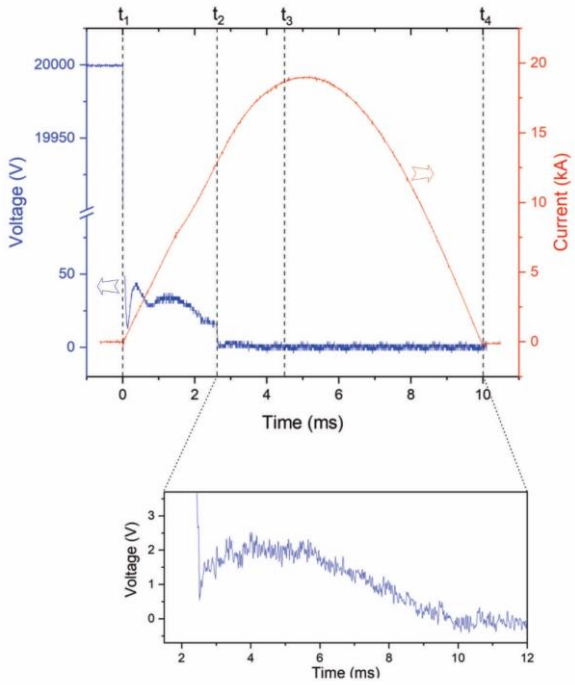

Figure 12. Typical current and voltage waveforms in a full making operation (arcing time: t_1 - t_2; latching time: t_2 - t_3).

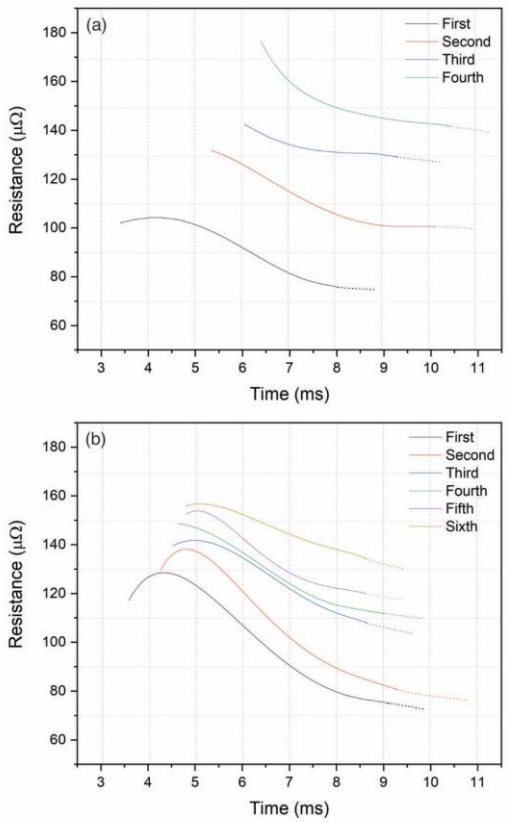

Figure 13. Arcing contacts' resistance in a series of operations under case 1 test conditions during latching time at a closing speed of 3 m/s (a) and 4 m/s (b)

total arc energy at different current levels causes approximately same contacts mass loss (Figure 7). The same results obtained for the electrodes fall energy are shown in Figure 8. However higher level of short-circuit current increases the probability of higher amount of dissipated energy, taking into account that the arcing time could not be longer than the first half-cycle of short-circuit current.

After the arcing contacts touch, the fault current continues to flow through the molten contacts, contributing to more energy dissipation. A part of current flows through the molten bridge between sliding contacts, which can further increase the dissipated energy and possibly contribute to the contact deterioration. While closing the switch, expansion of the molten zone between two sliding contacts [23] changes the contact resistance during latching time.

A closer view of the voltage waveform shows slight changes in the voltage after the abrupt jump associated with the arcing contact touch. Figure 12 shows the typical current and voltage waveforms for a making test where the voltage and current change during arcing (t_1-t_2) and latching (t_2-t_4) intervals. The resistance of moving contacts during latching interval is calculated for operations with just arcing contacts. Typical resistance profiles of sliding arcing contacts for successive tests with the current in case 1 at two closing speeds are shown in Figure 13. In a separate measurement, the contacts' resistance in the closed position of the switch is assessed as being in the range of 300 - 350 μΩ without passing short-circuit current. As shown in Figure 13, the resistances for both closing speeds are less than the steady state cold resistance of the main contacts. This is because of the increased effective contacts area provided by the molten metal on the contacts' surfaces. However, the deterioration of the arcing contact surfaces by repeating the operations makes the contacts' surfaces rougher, and changes the contact diameter, resulting in an increase of the measured resistances.

To evaluate the impact of energy dissipated by ohmic losses on arcing contacts welding, an equivalent circuit at the stage of arcing contacts touching, and the position where the main contacts approach, if this exists, is considered as shown in Figure 14 (a) and (b) respectively. r_c is the resistance of the contacts' touchpoint where the surface temperature is highest (and the surface is most probably molten) due to exposure to the pre-strike arc, and R(t) is the total resistance between the switch contacts. Therefore, the current flowing through the contacts' touchpoint (i_c) is defined as follows:

$$i_c(t) = i(t) \cdot \frac{R(t)}{r_c} \tag{6}$$

where i(t) is the total current flowing through the switch, r_c is the resistance of the touchpoint at t_2 determined from the resistance profile. Consequently, the energy dissipated (Ohmic losses) when the arcing contacts touch is described as follows:

$$E_c = \int_{t_2}^{t_4} r_c \cdot i_c^2(t) \cdot dt = \int_{t_2}^{t_3} \frac{R_1^2(t)}{r_c} \cdot i^2(t) \cdot dt + \int_{t_3}^{t_4} \frac{R_2^2(t)}{r_c} \cdot i^2(t) \cdot dt \tag{7}$$

where R_2(t) and R_1(t) are the total resistance between the switch contacts with and without main contacts, respectively. Table 1 shows detailed values of time intervals during arcing and latching stages for one of the measured series. The ohmic loss is calculated for each case. It can be seen by the increase in arcing time after each test, t_2-t_3 is going to be smaller, which indicates the arcing contacts erosion shown in figures 6, 7, and 10. The reduction continues until t_2 becomes equal to t_3, which means the arc still burns between arcing contacts when the main contacts touch (if exist). That is the reason of observed erosion

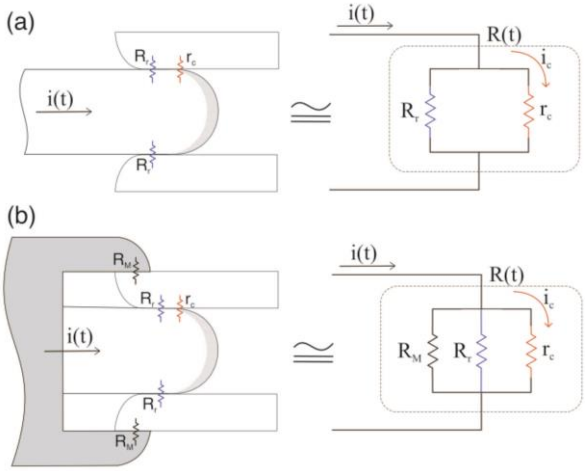

Figure 14. Schematic of the switch in closed position and the equivalent circuit with arcing contacts (a) and arcing and main contacts (b).

Table 1. Making operation time intervals and Ohmic losses at two closing speeds (3 and 4 m/s) with arcing contacts at case 1.

Closing speed	Test #	t_{arcing} (ms)	$t_{latching}$ (ms)		E_c (j)		E_T (j)
			t_2-t_3	t_3-t_4	t_2-t_3	t_3-t_4	
3 m/s	1	3.4	1.15	4.35	62.9	38.7	106.8
	2	5.3	0.73	5.17	46.1	126.2	196.03
	3	6.1	-*	4.23	-	90.4	96.4
	4	6.4	-*	5.1	-	182.2	208.8
4 m/s	1	3.6	0.68	5.82	29.07	131.6	171.4
	2	4.2	0.77	5.93	43.98	156.5	225.07
	3	4.5	0.32	4.98	17.15	133.7	157.7
	4	4.6	0.33	4.87	16.5	121.5	153.5
	5	4.8	-*	5.29	-	139.2	153.06
	6	4.8	-*	5.06	-	134.4	140.2

*. at this timing, t_2 would be equal to t_3

in main contacts mentioned in section III. B. Figure 14 (b) shows the schematic circuit of the switch in closed position if the main contacts are involved. In this case, R_m is the resistance of the main contacts in closed position, which is considerably smaller than r_c. Therefore, if the main contacts exist in the switch, most of the current passes through them, increasing the switch service life from four series of operations to seven times based on the obtained results.

As discussed in section II. A. these series of experiments are designed to reach the highest pre-strike arcing time, which occurs at a symmetrical current waveform. However, in real situations, the switch would be closed randomly, resulting in an asymmetrical current waveform. Equation 8 shows the destructive joule heating energy that causes switch failure in both forms of current waveforms (symmetrical and asymmetrical) includes pre-strike arc energy (E_{arc}) and ohmic loss energy (E_{OL}) which are described in detail in the previous sections

$$E_{destructive} = E_{arc} + E_{OL} = \int_{t_1}^{t_2} i_{arc}.V_{arc}.dt + \int_{t_2}^{t_4} i_c^2(t).r_c.dt \quad (8)$$

Referring to the results shown in Figure 6 and Table 1, E_{arc} is much higher than E_{OL}. Therefore, if no arc burns between the arcing contacts in the first half-cycle of the short-circuit current, the ohmic loss is not sufficiently high to cause switch malfunction. Therefore, it can be concluded that the most destructive impact of making operation on switch function occurs in the first half-cycle of short-circuit current, in which the pre-strike arc forms and the short circuit current flows through the sliding arcing contacts before the main contacts touch. Therefore, extending the obtained results in the present study to making tests combined with the rated short-time withstand current of 0.2 s (IEC 62271-103 [24]) is valid.

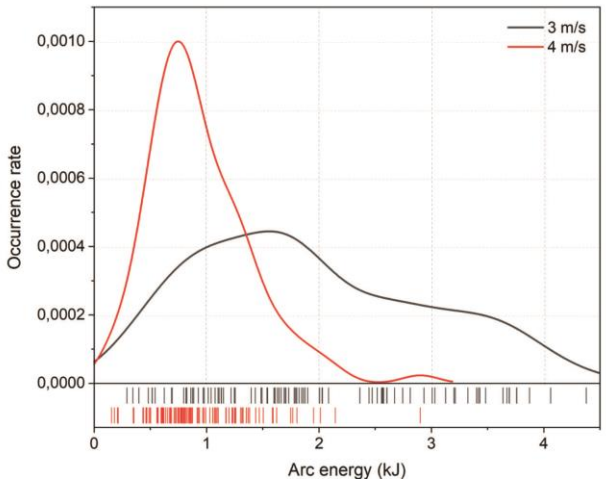

Figure 15. Distribution of the pre-strike arc anergy in case 1 with arcing contacts for closing speed of 3 and 4 m/s

The presence of main contacts in addition to arcing contacts in LBS could prolong the switch service life, as shown in figures 9 and 10. However, it is not the final solution since the arcing contacts welding occurred after seven successive making operations (case I). Increasing the closing speed is one of the solutions to reduce the impact of pre-strike arc on switch failure in making operation. The results show a slower rate of mass loss and less dissipated arc energy, with increasing the closing speed shown in the histogram graph in Figure 15. The increase in the closing speed decreases the pre-strike arc dissipated energy and arcing contact wear. Therefore, the rate of increase in the resistance is slower for the higher closing speed. However, there are other methods to decrease the arcing time like using pressurized insulation gas or different types/mixtures of insulation gas with superior insulation properties.

V. Conclusion

The making operation at different fault conditions is investigated for air-based MV-LBS. The factors and parameters involved in operations are evaluated based on synthetic testing, which is equivalent to direct testing. The following are the main findings of this study:

- The higher the pre-strike arcing time and current, the higher the dissipated arc energy between the contacts while closing.
- Arcing contacts' mass loss is mainly dependent on pre-strike arcing.
- The model switch failed to re-open due to arcing contacts welding after four successive making operations without main contacts and after seven successive operations with main contacts with a short circuit peak current of 22 kA and a breakdown voltage of 20 kV.
- The destructive energy responsible for the degradation of contacts during the pre-strike arc is much higher than the Ohmic losses caused by the fault current flow through the sliding contact
- Having the main contacts in the model switch can prolong the switch service life by reducing the Ohmic losses between arcing contacts in the closed position.
- The most destructive effects of the making operation occur in the first half-cycle of the short-circuit current (when the pre-strike arc burns). Hence, the results of this study can be extended to longer fault currents.
- Increasing the closing speed reduces the pre-strike arcing time and the rate of increase of sliding contact resistance during the latching interval.

VI. Acknowledgment

This work is financially supported by the Norwegian Research Council, grant # 269361. The authors would like to thank Marius Strand for his contribution in carrying out the experiments, and Bård Ålmos, Morten Flå, and Dominik Häger from NTNU for technical support.

VII. References

[1] N. Hatziargyriou and I. P. de Siqueira, *Electricity supply systems of the future*. Springer Nature, 2020.

[2] M. Seeger, R. Smeets, and J. Yan, "Recent development of alternative gases to SF6 for switching applications," *ELECTRA (cigre)*, 2017.

[3] M. Bendig and M. Schaak, "Design Rules for Environmentally Friendly Medium Voltage Load Break Switches," *IEEE Transactions on Power Delivery*, 2020.

[4] M. Taki, D. Maekawa, H. Odaka, H. Mizoguchi, and S. Yanabu, "Interruption capability of CF/sub 3/I Gas as a substitution candidate for SF/sub 6/gas," *IEEE Transactions on Dielectrics and Electrical Insulation*, vol. 14, no. 2, pp. 341-346, 2007.

[5] X. Li, H. Zhao, and A. B. Murphy, "SF6-alternative gases for application in gas-insulated switchgear," *Journal of Physics D: Applied Physics*, vol. 51, no. 15, p. 153001, 2018.

[6] N. S. Støa-Aanensen, M. Runde, E. Jonsson, and A. Teigset, "Empirical relationships between air-load break switch parameters and interrupting performance," *IEEE Transactions on Power Delivery*, vol. 31, no. 1, pp. 278-285, 2016.

[7] *IEC 62271-200: AC metal-enclosed switchgear and controlgear for rated voltages above 1 kV and up to and including 52 kV*, 2021.

[8] H. Taxt, K. Niayesh, and M. Runde, "Self-Blast Current Interruption and Adaption to Medium-Voltage Load Current Switching," *IEEE Transactions on Power Delivery*, vol. 34, no. 6, pp. 2204-2210, 2019.

[9] H. Taxt, K. Niayesh, and M. Runde, "Medium-voltage load current interruption in the presence of ablating polymer material," *IEEE Transactions on Power Delivery*, vol. 33, no. 5, pp. 2535-2540, 2018.

[10] E. Jonsson and M. Runde, "Interruption in air for different medium-voltage switching duties," *IEEE Transactions on Power Delivery*, vol. 30, no. 1, pp. 161-166, 2014.

[11] K. Niayesh and M. Runde, *Power Switching Components*. Cham, Switzerland: Springer, 2017.

[12] J. Tepper, M. Seeger, T. Votteler, V. Behrens, and T. Honig, "Investigation on erosion of Cu/W contacts in high-voltage circuit breakers," *IEEE transactions on components and packaging technologies*, vol. 29, no. 3, pp. 658-665, 2006.

[13] T. Cheng, W. Gao, W. Liu, and R. Li, "Evaluation method of contact erosion for high voltage SF6 circuit breakers using dynamic contact resistance measurement," *Electric Power Systems Research*, vol. 163, pp. 725-732, 2018.

[14] Y. Wu *et al.*, "Visualization and mechanisms of splashing erosion of electrodes in a DC air arc," *Journal of Physics D: Applied Physics*, vol. 50, no. 47, p. 47LT01, 2017.

[15] P. G. Slade, *Electrical contacts: principles and applications*. CRC press, 2017.

[16] J. J. Shea, "Erosion and resistance characteristics of AgW and AgC contacts," *IEEE Transactions on Components and Packaging Technologies*, vol. 22, no. 2, pp. 331-336, 1999.

[17] *IEC 62271-101: Synthetic testing*, 2021.

[18] N. Dorraki and K. Niayesh, "Optical investigation on pre-strike arc characteristics in medium-voltage load break switches," *Journal of Physics D: Applied Physics*, vol. 54, no. 25, p. 255503, 2021.

[19] Y. Yokomizu, T. Matsumura, R. Henmi, and Y. Kito, "Total voltage drops in electrode fall regions of, argon and air arcs in current range from 10 to 20 000 A," *Journal of Physics D: Applied Physics*, vol. 29, no. 5, p. 1260, 1996.

[20] M. Mohammadhosein, K. Niayesh, A. A. Shayegani-Akmal, and H. Mohseni, "Online assessment of contact erosion in high voltage gas circuit breakers based on different physical quantities," *IEEE Transactions on Power Delivery*, vol. 34, no. 2, pp. 580-587, 2018.

[21] A. Bagherpoor, S. Rahimi-Pordanjani, A. A. Razi-Kazemi, and K. Niayesh, "Online condition assessment of interruption chamber of gas circuit breakers using arc voltage measurement," *IEEE Transactions on Power Delivery*, vol. 32, no. 4, pp. 1776-1783, 2016.

[22] M. Iwata, T. Ohtaka, Y. Kuzuma, and Y. Goda, "Development of a method of calculating the melting characteristics of OPGW strands due to DC arc simulating lightning strike," *IEEE transactions on power delivery*, vol. 28, no. 3, pp. 1314-1321, 2013.

[23] C.-y. Zhu and B.-m. Li, "Analysis of sliding electric contact characteristics in augmented railgun based on the combination of contact resistance and sliding friction coefficient," *Defence Technology*, vol. 16, no. 4, pp. 747-752, 2020.

[24] *IEC 62271-103: Switches for rated voltages above 1 kV up to and including 52 kV*, 2021.

VIII. Biographies

Naghme Dorraki received the B.Sc. degree in optics and laser engineering from the University of Tabriz, Tabriz, Iran, in 2011, and the M.Sc. degree in photonics from the Laser and Plasma Research Institute, Shahid Beheshti University, Tehran, Iran, in 2015. She is currently pursuing the Ph.D. degree with the Department of Electric Power Engineering, Norwegian University of Science and Technology (NTNU), Trondheim, Norway. Her main interests are diagnosis of power switching components and plasma-material interactions.

Kaveh Niayesh (Senior Member, IEEE) received the B.Sc. and M.Sc. degrees in electrical engineering from the University of Tehran, Tehran, Iran, in 1993 and 1996, respectively, and the Ph.D. degree in electrical engineering from the RWTH- Aachen University of Technology, Aachen, Ger- many, in 2001. In the last 19 years, he held different academic and industrial positions including Principal Scientist with the ABB Corporate Research Center, Baden-Dättwil, Switzerland; Associate Professor with the University of Tehran; and Manager, Basic Research, with AREVA T&D, Regensburg, Germany. Currently, he is a Professor with the Department of Electric Power Engineering, Norwegian University of Science and Technology (NTNU), Trondheim, Norway. His research interests are mainly in the broad field of high voltage and switchgear technology; specifically on current interruption in power switching devices in ac and dc power networks, breakdown and aging behavior of insulation materials exposed to HVDC and repetitive fast impulses, as well as diagnostic and condition assessment of power switchgear.